Near Surface Geophysics, 2008, 327-332

The use of GPR to detect active layer in young periglacial terrain of Livingston Island, Maritime Antarctica

Georg Schwamborn*, Dirk Wagner and Hans-W. Hubberten

Alfred Wegener Institute for Polar and Marine Research, Telegrafenberg A43, 14473 Potsdam, Germany

Received July 2007, revision accepted August 2008

ABSTRACT

The South Shetland Islands offer ice-free margins with periglacial surfaces that are only a few decades old after the recent glacier retreat. Ground-penetrating radar (GPR) profiling was used to acquire information on young permafrost occurrence as deduced from active layer advance. Local GPR measurements included grids of parallel single-offset 2D reflection profiles and multi-offset measurements to determine wave velocity in the ground. Excavations served to determine the sedimentary composition and to backup GPR profile interpretation. GPR results show that the active layer could easily be traced at a site 140 m above sea level (asl), which is placed in volcanic soil. In contrast, GPR data were ambiguous at a site low in altitude (35 m asl), where frozen and unfrozen ground was imaged next to each other and GPR interpretation relied on ground verification.

INTRODUCTION

The past decades of permafrost research in Antarctica have seen several attempts to describe and comprehend permafrost occurrence but the knowledge is still limited to those individual studied geographic areas as summarized by Bockheim (1995) and Bockheim and Hall (2002). The Working Group within the International Permafrost Association (IPA) and the Expert Group within the Scientific Committee on Antarctic Research (SCAR) have encouraged future initiatives on (among others) acquiring spatial information on permafrost form, temperature and moisture content throughout the Antarctic region. The CALM (Circumpolar Active Layer Monitoring) program provides a database, where data are gathered on active layer depths of both Arctic and Antarctic permafrost sites (Brown *et al.* 2000). In the frame of the IPY (International Polar Year) 2007/8 one of the permafrost related projects (Permafrost Observatory Project: A Contribution to the Thermal State of Permafrost) (Activity ID No: 50) is devoted to increase the number of boreholes and active layer observational sites, which is represented for Antarctica through the ANTPAS (Antarctic Permafrost and Soil) initiative. The common aim of the initiatives is to understand the environmental conditions explaining the spatial distribution of permafrost, its properties and related processes to overcome gaps of knowledge.

Fieldwork should be planned and systems designed with regards to what kind of sub-surface is being measured. For coarse-grained slope debris as found on Hurd Peninsula, central Livingston Island (Fig. 1b), an active layer monitoring has been established by drilling boreholes to study the thermal regime (Ramos and Vieira 2003). Measuring temperature profiles in Maritime Antarctica following the CALM protocol is established for example at King George Island and Signy Island (Cannone *et al.* 2006).

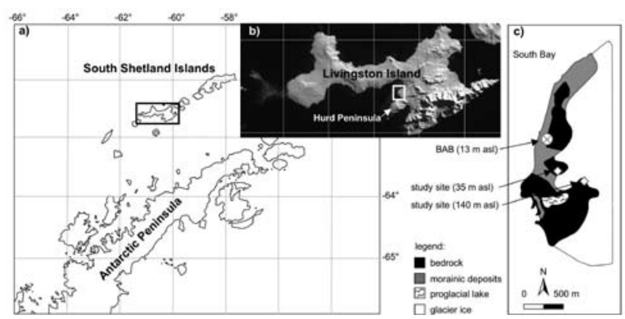

FIGURE 1
a) Geographical setting and b) SPOT satellite image of Livingston Island, c) (enlarged box of b) position of the study sites in the vicinity of the Bulgarian Antarctic Base (BAB). The mapped surfaces are simplified from Lopez-Martinez *et al.* (1992). ‘Bedrock’ includes surface debris that results from glacier reworking and slope processes in the area. The circle marks the position of the BAB, the triangle marks the study site in the field.

Geophysical techniques are considered a valuable complementary tool for visualizing permafrost construction, i.e., reflection seismic profiling and electrical resistivity (Kim *et al.* 1996; Hauck *et al.* 2007), or geoelectric sounding (Guglielmin *et al.* 1997). Specifically GPR has been used successfully to achieve insights into the near-surface structure of frozen ground (Doolittle *et al.* 1990) and to map active layer thickness along transects (Hinkel *et al.* 2001). With careful local calibration, usually accomplished through digging or coring, estimates on thaw depth along continuous profiles can be made.

*georg.schwamborn@awi.de

This paper contributes to fill the gap by exploration geophysical means (i.e., ground penetrating radar) to support active layer observations in Antarctica. Our objective was to identify the permafrost table in a dynamic periglacial setting. The approach was to acquire continuous GPR profiles as a tool to determine the transition from frozen to unfrozen ground. We considered environmental factors such as topographic setting and substrate, which potentially influence the preservation of perennial frozen ground.

The distribution and properties of permafrost in ice-free areas of the Antarctic margins influence the evolution of the microbial communities in Antarctic soil. The presented study forms an important data basis for an accompanying study to comprehend the functional microbial diversity in extreme Antarctic habitats (Wagner *et al.* 2006).

STUDY AREA

Livingston Island is the second largest among the South Shetland Islands, Maritime Antarctica (Fig. 1a). The area has 845 km^2, only 10% of which is ice and snow free in the period of the austral summer. Three physiographic sectors can be distinguished on the island; the eastern sector is covered by mountain glaciers, the central is characterized by ice domes and plateaus and the western sector is a plain almost ice free (Fig. 1b). Detecting sedimentary permafrost was accomplished in the vicinity of the Bulgarian Antarctic Base (BAB), which is located north of Hurd Peninsula, central Livingston Island (S 62°38'24", W 60°21'36"). The ice free high coast of the BAB is 2.5 km in length and 0.2 km to 0.3 km in width (Fig. 1c). It shows mainly morainic lobes, debris infilled depressions, debris cones and gelifluction lobes next to outcropping Cretaceous sandstones and Tertiary crystalline rocks (Smellie *et al.* 1995; Pimpirev *et al.* 2000). Raised beaches on the coast are developed below the height of 20 m asl. (Lopez-Martinez *et al.* 1992; Pallas *et al.* 1993). There is widespread volcanic fallout, which is related to explosions of the nearby Deception Volcano (Calvet *et al.* 1993). Numerous dark ash layers are distinct in glacier formations and the mainly lapilli-sized grains form residual melt out patches in the glacier fore-fields or are mixed into other surface debris.

Geomorphological mapping in the early 1990s shows that the ice margin has been retreating for several tens of metres since 1990–91 (Lopez-Martinez *et al.* 1992). This is a common feature in the Antarctic Peninsula and the surrounding islands for the last six decades due to atmospheric warming (Cook *et al.* 2005). For example, the 'proglacial lake' in the lower part of Fig. 1(c) was originally mapped as glacier ice (Lopez-Martinez *et al.* 1992). The ice has vanished now and turned to a small proglacial lake exposed in a cirque-shaped depression. Ice-bearing moraines in the glacier fore-field at BAB are common, as indicated in the GPR profiles and exposures (Schwamborn 2006) and they show considerable thawing during the austral summer season. Within weeks this process can cause a subsidence of several decimetres. The GPR shows strong reflection responses at the contact zone between the plateau glacier ice and the bedrock underneath, which suggests the presence of water at the ice-bed interface, as is typical for temperate glaciers (Navarro *et al.* 2005). With apparently no frozen ground underlying the glaciers and the high rate of glacial retreat (100 m within 15 years) we expect the permafrost in the glacier fore-field to be a young feature.

Meteorological records measured in the South Shetland Islands account for a cold maritime climate with the annual isotherm -2°C close to the sea level and mean-monthly values above 0°C from December to March (Serrano and Lopez-Martinez 2000 and references cited therein). Mean annual precipitation is about 500 mm (Vieira and Ramos 2003). Temperature measurements taken at the BAB during three austral campaigns (1993–1996) show a maximum summer temperature of 7.5°C, the minimum winter temperature was -24°C. Permafrost can be expected above the Holocene raised-beaches, where borehole results on Hurd Peninsula show that the permafrost table occurs below an active layer of 230 cm depth at 35 m asl and below 50 cm to 100 cm depth at 275 m asl (Ramos and Vieira 2003).
GPR data acquisition took place at two selected sites (140 m asl and 35 m asl, Fig. 1c) where fine-grained soils allowed pulling the antenna continuously across the terrain, thus providing fairly good ground coupling.

DATA ACQUISITION

The theory and practical use of GPR has been covered in several publications (Annan and Davis 1976; Daniels *et al.* 1988). Profiling near surface structures with GPR is done by recording reflections between materials showing a contrast in dielectric permittivity ε. The permittivity of ground materials is partly determined by its dry characteristics (e.g., grain size changes, porosity) and partly by its ice or water contents (Annan and Davis 1976; Davis and Annan 1989; Daniels *et al.* 1988; Arcone *et al.* 1998). Permafrost usually has an ε of 4–5, whereas saturated soil can reach an ε of 40. The permittivity is a measure of the polarizability of a material, which is mainly influenced by the presence of liquid water. With increasing penetration the radar impulse is attenuated due to wave spreading and material absorption.

We used a RAMAC impulse radar and 200 MHz, 100 MHz and 50 MHz antenna pairs, a trigger unit and a field PC for direction. We acquired single-offset and multi-offset GPR records along grids of parallel lines. Multi-offset measurements were acquired for estimating the wave velocity in the ground. The multi-offset mode allows hyperbola fitting in the radargram in order to convert traveltimes to depth. Only 200 MHz records were found useful to image dm-scale soil features in areas, which are surrounded by bedrock outcrops or coarse-grained slope debris. Lower frequency profiles suffer from a lack of coherent reflections in the weathering debris covering the bedrock in layers of usually less than one metre.

The ground-loaded pulse period of our 200 MHz records was 15 ns with an actual centre frequency decreased down to 150 MHz in average. Assuming that reflection events half of the pulse length, 1 1/2 cycles can be traced at best in these records,

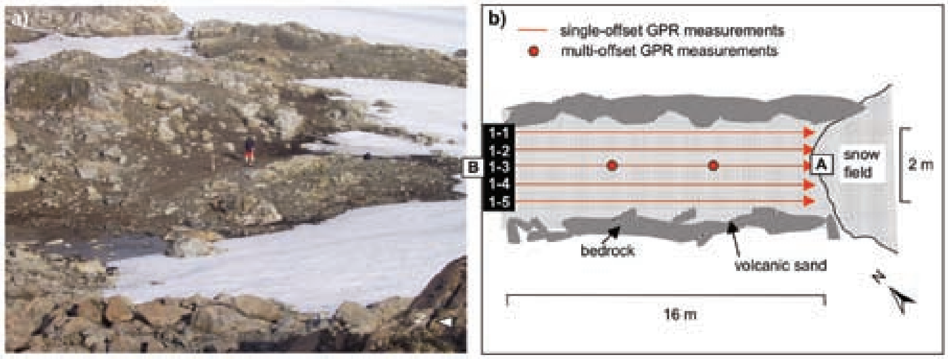

FIGURE 2
a) Photograph of the study site at 140 m asl. Note the snowfield that borders one end of the site. b) The profile grid had several parallel lines and two centrally located points of velocity measurements. Results of the left measuring point are displayed in Fig. 3. Parallel lines are displayed in Fig. 4.

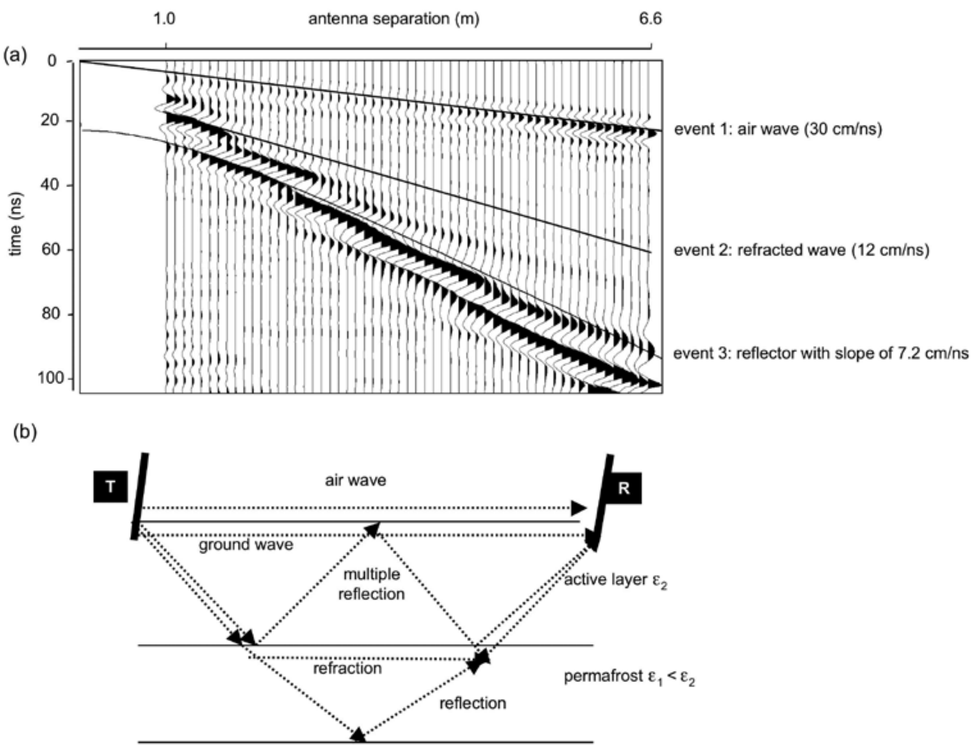

FIGURE 3
a) A multi-offset record to calculate wave velocities in the ground. The transmitter and receiver have been separated at equal intervals of 10 cm. This produces a separation versus traveltime plot. b) Shows the principal radar travel paths that can be expected in the active layer and near surface permafrost (see also Arcone and Delaney 2003).

this yields a vertical resolution of about 40 cm in unfrozen sediments. This estimate uses an active layer velocity of 5 cm/ns (e.g., Moorman *et al.* 2003).

In addition, direct measurements of the depth to an observed radar reflector have been performed with excavating soil to convert observed 2-way signal traveltimes directly to velocities. All GPR and excavation measurements were completed mid-February 2005 preceding the average freezing period lasting from March to October (Ramos and Viera 2003).

Post-processing was applied to the radar data to improve the visibility of the radargrams. We applied a DC subtraction to remove the initial low-frequency content and a bandpass filter to remove high-frequency noise. A gain function strengthened the low amplitude reflections, a horizontal mean filter smoothed the wavelet appearance and a static correction accounted for the time zero onsets.

RESULTS AND DISCUSSION

At the site 140 m asl (S 62°38’50”, W 60°21’39”, Fig. 1c) volcanic sands within outcropping Cretaceous sandstones fill an elongated depression that is 16 m in length and 2 m in width (Fig. 2a). A retreating snowfield confined the SE margin of the measuring site during the field studies. The survey grid in the volcanic soil comprised five parallel lines and two centrally positioned points of data collection in the multi-offset mode (Fig. 2b).

The velocity measurements recorded with 200 MHz antennas (antenna offset: 0.6 m) show a succession of several time delay events between the transmitter and the receiver antenna (Fig. 3). Whereas the airwave, which is the first response to arrive and which gives the value for the speed of light (30 cm/ns), is clearly visible (event 1 in Fig. 3a), the second event seems to result from the refracted wave giving a velocity of 12 cm/ns from the top of the permafrost. This event precedes the direct wave and can generally be followed by dispersive guided waves. The third arrival (event 3) is interpreted as the response from a reflector in the ground yielding a wave velocity of 7.2 cm/ns. This value is typical for an unfrozen soil layer on top of a subground separated by a sufficiently high dielectric contrast. Converted to depth this points to a reflector about 81 cm deep. If the signal return results from multiple propagation, the reflector could be generated from an interface half that deep (see Fig. 3b). Figure 4 displays the active layer depth as measured by continuous GPR lines. A first continuous high amplitude event between 10 and 20 ns two-way traveltime (TWTT) can be traced clearly, especially in lines 1–1, 1–2 and 1–3. The reflector rises up at each end of the profiles, though more uniformly visible at the SE ends. Here, the first reflection also merges with the ground wave.

12 ns TWTT down to the first reflector in the centre part of the lines accounts for an active layer depth of about 43 cm. This uses a wave velocity of 7.2 cm/ns as deduced from the multi-offset measurement. Related to the velocity measurements (Fig. 3a) this would argue that the slope showing that velocity, results from multiple reflections (event 3). Active layer delineation is distinct in lines 1–1, 1–2 and 1–3. However, there are more continuous reflections present down to 30 ns TWTT, partly also with more internal structuring (Fig. 4, 1–4). In contrast, line 1–5 loses continuity of reflections, especially to the lower end of the upper unit. The lower unit is characterized by the absence of continuous reflections. Presumably, the lower unit represents the bedrock underlying the volcanic sands.

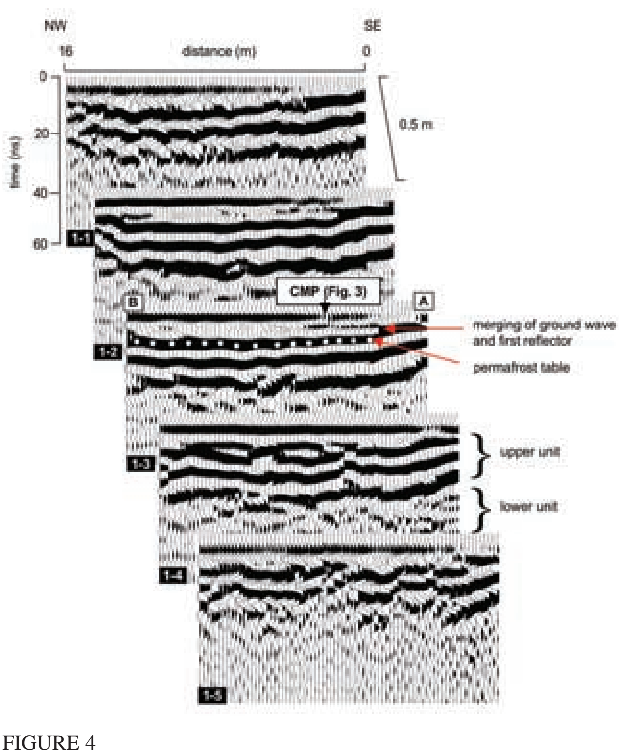

FIGURE 4
Several single-offset lines across the site at 140 m asl. The continuous first reflections indicate active layer. The lower unit is interpreted to mark the transition from sedimentary fill to bedrock.

Along the A to B profile (line 1–3) the soil was excavated immediately after the GPR data collection. The volcanic soil had an active layer depth of 40 cm at maximum in the mid of February 2005 (Fig. 5) and consisted mostly of a sandy substrate that has slightly coarser portions in the top few centimetres. The bottom part of the active layer at the B-end contained weathering debris derived from the sandstone that frames the site. At the A-end the soil was water saturated where the active layer pinched out towards the adjacent snowfield. This is the location, which shows a merging of the ground wave and the first reflector in line 1–3 (Fig. 4). It suggests that the late retreat of the seasonal snow cover has delayed the frozen ground from thawing. In the middle part of the excavation profile there is a fairly good matching of the directly measured active layer depth in the excavation (34 cm) with the result calculated from the velocity depicted from the multi-offset panel of Fig. 3 (43 cm) accepting common resolution limits of the used frequency.

The second site at 35 m asl (S 62°38'24", W 60°21'36") (Fig. 1c) is also placed in volcanic soil framed by outcropping rocks. Three parallel 200 MHz GPR lines measure 15 m in length and have a distance of 0.5 m in between (Fig. 6). The site was snow free at the time of the measurements in mid February. The three lines exhibit strong continuous reflections down to about 20 ns TWTT before reflection coherence is lost. Inclined reflections interpreted as diffraction hyperbolas caused by bedrock mark the NE ends. The lines 2–2 and 2–3 have elliptic features in the central profile parts at about 10 ns TWTT, bigger in line 2–2, smaller in 2–3.

Subsequent digging of the soil revealed that the upper ground (25–30 cm) was composed of volcanic soil overlying a clay-containing diamicton, which is interpreted as till. Both sandy top layers and the till underneath were unfrozen. However, in the centre part the soil had frozen sand below a thin unfrozen layer of 5 cm. This frozen portion fairly well matches the position of the elliptic features pronounced in the radargrams. We thus interpret that these ellipses represent the frozen ground.

The borehole temperature data from the nearby ice-free margin on Hurd Peninsula (3 km away) demonstrate that a low altitude site (35 m asl) is influenced by the thermal inertia of the seawater. This results in a thick active layer more than 230 cm

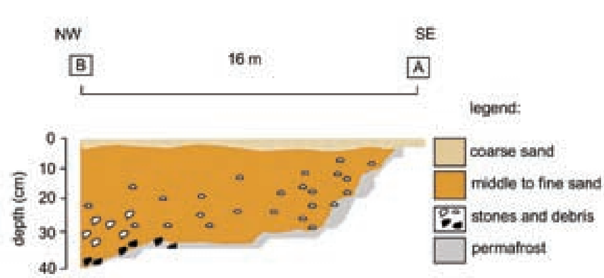

FIGURE 5
Sketch of digging results along GPR line 1–3.

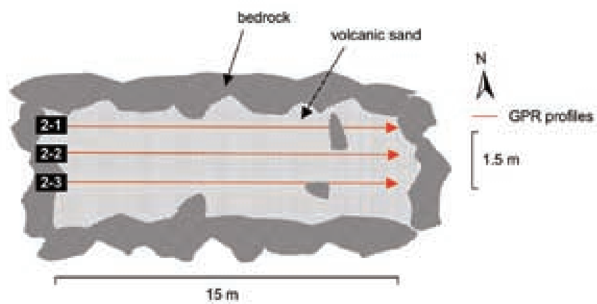

FIGURE 6
Sketch of the study site at 35 m asl. It is placed in volcanic soil that is framed by outcropping rock.

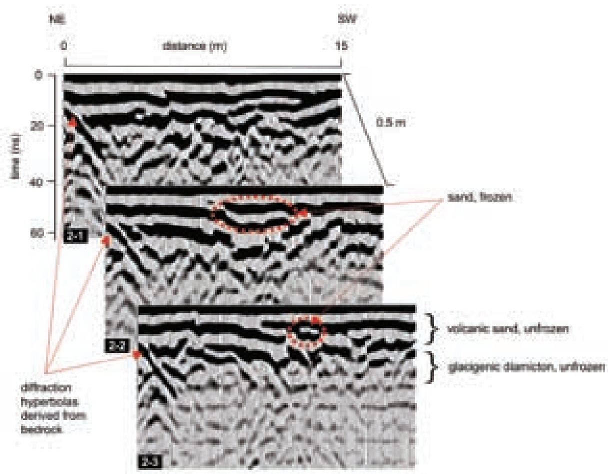

FIGURE 7
Three parallel GPR profiles across the site at 35 m asl. Dashed ellipses highlight patches of frozen ground.

deep (Ramos and Vieira 2003), a depth that is not captured by the GPR signal penetration studied here.

The cause for encountering frozen ground in an otherwise unfrozen environment is seen to be analogueous to site one, where a late retreating snow cover may have delayed the ground thawing. The patchy frozen ground encountered at the site may thus only be a short-term event.

Both experimental sites show several local effects likely related to inhomogeneous snow retreat, terrain heterogeneity, hill creep and variations in glacial run-off and infiltration, which strongly affect the thawing process. These exogenic near surface conditions on a slope may change annually. Furthermore, endogenic processes such as frost heave, cryoturbation or other soil sorting processes can add to alter physical conditions. All the factors create a small-scale mosaic of soil with variable grain fabric and variable water and ice contents. Alternative techniques such as electrical resistivity sounding and refraction seismics (Hauck *et al.* 2007) can provide complementary data sets on the distribution of permafrost. However, they usually lack precise depth information and do not allow distinguishing between inherited frozen ground and recently formed permafrost that is related to modern climate conditions.

The small-scale variability of permafrost distribution and properties in the study area has a crucial effect on the structure and function of the microbial communities in these ecosystems. For comparison, Siberian permafrost has well adapted microbial communities along the extreme temperature gradient in the active layer. Two different populations of methane oxidizing bacteria are reported with different physiological characteristics (mesophilic or cold-adapted; Liebner and Wagner 2006). Due to their physiological adaptation permafrost microorganisms form specific phylogenetic clusters (Ganzert *et al.* 2006). For ongoing studies on the functional diversity and the response of microbial communities to global climate changes the knowledge on the present permafrost status in Livingston Island and its future development is of special interest.

CONCLUSIONS

Determining the active layer thickness at a site 140 m asl by GPR was accurate when compared with ground verification. At a site lower in altitude (35 m asl) GPR results were not conclusive in their own. Instead, patchy frozen ground was identified only after excavation.

Detecting young permafrost by GPR means alone remains challenging when applied in geomorphologically highly dynamic settings at glacier margins. Areas such as the South Shetland Islands and other environments, which are deglaciated only recently, need more sources of information such as digging, coring or supplementary geophysics to confirm permafrost.

Active layer monitoring has to be acted with caution when done in newly formed permafrost within young periglacial terrain and in slope settings, since the thermal regime of soil layers is affected by surface reworking due to glacial run-off and annually changing snow covers that will induce changing insulation effects.

ACKNOWLEDGEMENTS

We express our strong gratitude to our colleagues at the Bulgarian Antarctic Base St. Kliment Ohridski, namely Christo Pimpirev, Mihail Vajarov and Jordan Radkov Yankov. They provided essential logistical support in the field. Our thanks are extended to the Spanish crew of MV 'Las Palmas' (Armada Espanola) for performing the seaway transfer.

REFERENCES

Annan A.P. and Davis J.L. 1976. Impulse radar sounding in permafrost. *Radio Science* **11**, 383–394.

Arcone S.A. and Delaney A.J. 2003. Radiowave pulse refraction and ground wave propagation through permafrost and the active layer. In: *Proceedings of the 8th International Conference on Permafrost* (eds M. Phillips, S. Springman and S.M. Arenson), pp. 21–25. Balkema Publishers, Lisse. ISBN 90 5809 5827.

Arcone S.A., Lawson D.E., Delaney A.J., Strasser J.C. and Strasser J.D. 1998. Ground-penetrating radar reflection of groundwater and bedrock in an area of discontinuous permafrost. *Geophysics* **63**, 1573–1584.

Bockheim J.G. 1995. Permafrost distribution in the Southern Circumpolar region and its relation to the environment: A review and recommendations for further research. *Permafrost and Periglacial Processes* **6**, 27–45.

Bockheim J.G.. and Hall K.J. 2002. Permafrost, active-layer dynamics and periglacial environments of continental Antarctica. *South African Journal of Science* **98**, 82–90.

Brown J., Hinkel K.M. and Nelson F.E. 2000. The Circumpolar Active Layer Monitoring (CALM) program: Research designs and initial results. *Polar Geography* **24**, 165–258.

Calvet J., Pallas R., Sabat F. and Vilaplana J.M. 1993. Los niveles de cenizas de los glaciares de Livingston – criterios para su adaptacion. In: *Actas del V simposio espanol de estudios Antarcticos. Comisión interministerial de ciencia y tecnologia* (eds J. Cacho and D. Serrat), pp. 195–208.

Cannone N., Ellis Evans J.C., Strachan R. and Guglielmin M. 2006. Interactions between climate, vegetation and the active layer in soils at two Maritime Antarctic sites. *Antarctic Science* **18**, 323–333.

Cook A.J., Fox A.J., Vaughan D.G. and Ferrigno J.G.. 2005. Retreating glacier fronts on the Antarctic Peninsula over the past half-century. *Science* **308**, 541–544.

Daniels D.J., Gunton D.J. and Scott H.F. 1988. Introduction to subsurface radar. *IEE Proceedings F* **135**, 278–321.

Davis J.L. and Annan A.P. 1989. Ground-penetrating radar for high-resolution mapping of soil and rock stratigraphy. *Geophysical Prospecting* **37**, 531–551.

Doolittle J.A., Hardisky M.A. and Gross M.F. 1990. A ground-penetrating radar study of active layer thicknesses in areas of moist sedge and wet sedge tundra near Bethal, Alaska, USA. *Arctic and Alpine Research* **22**, 175–182.

Ganzert L., Jurgens G., Münster U. and Wagner D. 2006. Methanogenic communities in permafrost-affected soils of the Laptev Sea coast, Siberian Arctic, characterized by 16S rRNA gene fingerprints. *FEMS Microbiology Ecology* **59**, 476–488. doi:10.1111/j.1574-6941.2006.00205.x

Guglielmin M., Biasini A., Dramis F. and Smiraglia C. 1997. The contributions of geoelectrical investigations in the analysis of periglacial and glacial landforms in ice free areas of the northern foothills (northern Victoria Land, Antarctica). *Geografisker Annaler* **79A**, 17–24.

Hauck C., Vieira G., Gruber S., Blanco J. and Ramos M. 2007. Geophysical identification of permafrost in Livingston Island, maritime Antarctica. *Journal of Geophysical Research* **112**, F02S19. doi:10.1029/2006JF000544

Hinkel K.M., Doolittle J.A., Bockheim J.G., Nelson F.E., Paetzold R., Kimble J.M *et al*. 2001. Detection of subsurface permafrost features with ground penetrating radar, Barrow, Alaska. *Permafrost and Periglacial Processes* **12**, 179–190.

Kim Hyoung-Soo., Nam Sang Heon. and Kim Yeadong, 1996. Near surface geophysical surveys using seismic and electric methods in Barton Peninsula of King George Island, Antarctica. *Journal of Geological Society Korea* **32**, 131–145.

Liebner S. and Wagner D. 2006. Abundance, distribution and potential activity of methane oxidising bacteria in permafrost soils from the Lena Delta, Siberia. *Environmental Microbiology* **9**, 107–117. doi:10.1111/j.1462-2920.2006.01120.x

Lopez-Martinez J., Martinez de Pison E. and Arche A. 1992. Geomorphology of Hurd Peninsula, Livingston Island, South Shetland Islands. In: *Recent progress in Antarctic Earth Science* (ed. Y. Yoshida), pp. 751–756. Terra Scientific Publishing Co. (TERRAPUB), Tokyo.

Moorman B.J., Robinson S.D. and Burgess M.M. 2003. Imaging periglacial conditions with ground-penetrating radar. *Permafrost and Periglacial Processes* **14**, 319–329.

Navarro F.J., Macheret Y.Y. and Benjumea B. 2005. Application of radar and seismic methods for the investigation of temperate glaciers. *Journal of Applied Geophysics* **57**, 193–211.

Pallàs R., Vilaplana J.M. and Sàbat F. 1993. Anàlisis neotectónico de la península Hurd, isla Livingston. In: *Actas del V simposio espanol de estudios Antárcticos. Comisión interministerial de ciencia y tecnologia* (eds J. Cacho and D. Serrat), pp. 181–194.

Pimpirev C., Dimov D. and Miller H. 2000. Field studies of sedimentary sequences in Eastern Hurd Peninsula Central Livingston Island, South Shetland Islands. *Polarforschung* **66**, 1–5.

Ramos M. and Vieira G. 2003. Active layer and permafrost monitoring in Livingston Island, Antarctic. First results from 2000 to 2001. In: *Proceedings of the 8th International Conference on Permafrost* (eds M. Phillips, S. Springman and S.M. Arenson, S.M.), pp. 929–933. Balkema Publishers, Lisse. ISBN 9058095827.

Schwamborn G.. 2006. Permafrost verification on maritime Antarctica using ground penetrating radar. *Reports on Polar and Marine Research* **539**, 105–113.

Serrano E. and Lopez-Martinez J. 2000. Rock glaciers in the South Shetland Islands, Western Antarctica. *Geomorphology* **35**, 145–162.

Smellie J.L., Liesa M., Munoz J.A., Sabat F., Pallas R. and Willan R.C.R. 1995. Geological evolution of central Livingston Island, South Shetland Islands. *Antarctic Science* **7**, 99–113.

Vieira G. and Ramos M. 2003. Geographic factors and geocryological activity in Livingston Island, Antarctic. Preliminary results. In: *Proceedings of the 8th International Conference on Permafrost* (eds M. Phillips, S. Springman and S.M. Arenson), pp. 1183–1188. Balkema Publishers, Lisse. ISBN 9058095827.

Wagner D. 2006. Functional microbial diversity in extreme Antarctic habitats. *Reports on Polar and Marine Research* **539**, 98–104.